LETTER

Adhesionable flexible GaN-based microLED array film to brain surface for in vivo optogenetic stimulation

Applied Physics Express **15**, 046501 (2022) **LETTER**
https://doi.org/**10.35848/1882-0786/ac5ba3**

Adhesionable flexible GaN-based microLED array film to brain surface for in vivo optogenetic stimulation

Hiroto Sekiguchi[1,2*], Hayate Matsuhira[1], Ryota Kanda[1], Shuto Tada[1], Taiki Kitade[1], Masataka Tsutsumi[1], Atsushi Nishikawa[3], Alexander Loesing[3], Izumi Fukunaga[4], Susumu Setogawa[5], and Noriaki Ohkawa[5]

[1]*Department of Electrical and Electronic Information Engineering, Toyohashi University of Technology, Toyohashi, Aichi—441-8580, Japan*
[2]*Japan Science and Technology (JST), Precursory Research for Embryonic Science and Technology (PRESTO), Kawaguchi, Tokyo—102-0076, Japan*
[3]*ALLOS Semiconductors GmbH, Dresden 01237, Germany*
[4]*Sensory and Behavioural Neuroscience Unit, Okinawa Institute of Science and Technology Graduate University, Okinawa—904-0495, Japan*
[5]*Division for Memory and Cognitive Function, Research Center for Advanced Medical Science, Comprehensive Research Facilities for Advanced Medical Science, Dokkyo Medical University, Shimotsuga-gun, Tochigi—321-0293, Japan*

*E-mail: sekiguchi@ee.tut.ac.jp

Received February 13, 2022; revised February 26, 2022; accepted March 8, 2022; published online March 17, 2022

A development of a biocompatible, optical stimulation device capable of adhering to the brain surface and activating spatially separated brain regions is necessary for in vivo optogenetic applications. In this study, a hollow structure for isolating the microLED epitaxial layer was fabricated using the anisotropic KOH wet-etching method. Using a thermal release sheet, a method to transfer microLEDs onto a biocompatible parylene film was established without rotation or misalignment of the microLEDs while retaining their characteristics. Accordingly, a flexible microLED array film was fabricated, which adhered to the surface of the brain of a mouse and exhibited blue emission. © 2022 The Japan Society of Applied Physics

The high brightness, low power consumption, long life, and durability of GaN-based microLEDs make them suitable for many applications, such as smart fiber[1)] and Li-Fi high-speed data communication technologies[2,3)] as well as high-resolution and high-brightness displays.[4,5)] Particularly, microLED arrays capable of controlling neural activity are increasingly used in optogenetics technology.[6–8)] To understand brain function organized by complex neural network, it is necessary to optically stimulate multiple regions of the brain individually or simultaneously. It is difficult to achieve this using the conventional optical fiber method; therefore, an array of light sources is required. Although presentations of patterned light have been achieved in head-fixed animals using optical microscope,[9–11)] an implantable array of light sources is needed for investigations under more naturalistic conditions, such as in freely moving animals, and clinical applications. Several reports on the development of a microLED neural probe with a needle-shaped structure for accessing the deep brain region have been published.[12–17)] However, the development of a microLED array neural tool for activating spatially distributed brain regions at a mesoscale has not been sufficiently investigated. Therefore, if a biocompatible microLED array film that can adhere to the brain surface is developed, it would significantly contribute to the field of neuroscience and possibly clinical applications by functioning as a bioimplantable optical stimulation device.

It is necessary to develop a technology for accurately transferring and arranging microLEDs on a flexible film composed of biocompatible materials, such as parylene and polydimethylsiloxane. Regarding the transfer technology of microLED, the pick-and-release method using an elastomer stamp,[18–20)] laser-enabled advanced placement (LEAP) technology,[21,22)] and fluid alignment technology[23,24)] have been reported. However, as the modulation range of the adhesive force is limited while using an elastomer stamp, it is difficult to obtain a high transfer rate on a biocompatible film having no adhesive force. In the LEAP method, the biocompatible film melts or deteriorates owing to the heat generated by the laser, and in the fluid assembly method, it is difficult to form the groove required for self-assembly on a thin film. Therefore, to realize optogenetic multipoint stimulation, a microLED transfer technology that can achieve adhesion to the brain surface with a high success rate without causing a rotation or misalignment of the microLEDs and without damaging the thin and low-heat-resistant biocompatible film is required. In this study, the film thickness required for achieving contact with the brain surface was investigated, and a transfer technology using a TR sheet was established to fabricate a flexible microLED array film. The developed film adhered to the surface of the cerebral cortex of a living mouse and blue emission was observed.

Parylene C was selected as the base film for the microLED array owing to its robustness, flexibility, and biocompatibility. As the bending stiffness reduces upon decreasing the thickness of the film, a film with high adhesion can be realized. However, an ultrathin film is impractical because it would be mechanically fragile and would not sufficiently self-support during implantation. As it is important to determine the appropriate film thickness for the realization of flexible microLED films, the effect of the radius of curvature on adhesion was investigated by wrapping the film around different cylinders. The adhesion energy can be expressed as:

$$\gamma \geqslant \gamma_c = \frac{S}{2R^2 b}, \tag{1}$$

where γ_c, S, R, and b are the critical adhesion energy, bending stiffness, curvature radius, and width of the film, respectively.[25)] The S depends on the material properties and device structure. Therefore, for the formation of a metal wiring of 64 channels, 64 ch Ti/Au (50/200 nm) metal wirings of width 20 μm were applied on the surface of a 3 mm wide parylene sheet for the wrapping experiment. The experimental results depend on whether the interface is wet or dry. Physiological saline was used in the wrapping experiment to simulate the cerebrospinal fluid present on the surface of the brain resulting in a wet environment. Figure 1(a) shows the wrapping of 12 μm thick parylene sheets around glass cylinders of radii 0.4, 2, and 5 mm. The

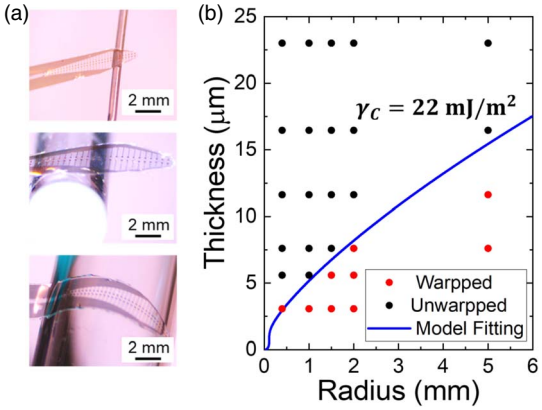

Fig. 1. (Color online) (a) Wrapping of 12 μm thick parylene sheets with 64 channel metal wiring around glass cylinders with radii of 0.4 (unwrapped), 2 (unwrapped), and 5 mm (wrapped). (b) Summary of wrapping experiment. Red and black circles represent wrapped and unwrapped data, respectively. The blue line represents the simulation line with $\gamma_c = 22$ mJ m^{-2} obtained from the mechanical model.

12 μm thick sheets did not wrap around the cylinders of radii 0.4 and 2 mm; however, they wrapped around the cylinder of radius 5 mm. Figure 1(b) shows a summary of the wrapping experiment plotted with respect to the cylinder radius and sheet thickness. Red and black circles represent the wrapped and unwrapped data, respectively. Thicker sheets adhered to cylinders of larger radii. The results were compared with those obtained using the mechanical model in Eq. (1). The S was calculated based on a multilayered structure containing the metal wiring of the device.[25] These results were in agreement with the simulated line; $\gamma_c = 22$ mJ m^{-2} was obtained, which corresponded with the value reported for a wet environment.[26] Considering these findings and the radius of curvature of a mouse's brain (approximately 4–5 mm), the parylene thickness was determined to be 11 μm, which provides sufficient adhesion and robustness.

Next, the transfer technology of the microLED array onto the parylene film was investigated. Figure 2(a) shows the fabrication procedure of a flexible microLED film. First, a hollow-structured microLED array was fabricated to release only the LED epitaxial layer for transferring onto the parylene film. An InGaN-based LED structure with an emission wavelength of 450 nm on a (111) Si substrate (ALOSS Semiconductors GmbH) was used.[27] The design consisted of 80 μm square microLEDs arranged in a 7×6 array on a 1 mm square. Prior to the fabrication of the array, a Ge-doped GaN layer (doping concentration: 2×10^{20} cm^{-3}) was deposited on the p-GaN layer by a sputtering system to form an np tunnel junction, resulting in a low contact resistance for the p-type GaN, and the device fabrication process was simplified using the same metal for both p- and n-electrodes. Using the circular transfer length method, an extremely low contact resistance excluding the tunnel junction resistance, within the range $1–2 \times 10^{-6}$ Ω·cm^2, was confirmed. A mesa structure was formed using an inductively-coupled, plasma-reactive ion etching for the n-contact, followed by the dry etching of the n-GaN layer around the microLED to the Si substrate. Here, two-step dry etching was important as excessive etching would promote plasma damage from the sidewall and significantly reduce the emission efficiency. Subsequently, Ti/Au (50 nm/200 nm) n- and p-electrodes were deposited using an electrode beam (EB) evaporator. To protect the GaN surface from the subsequent KOH solution etching, a 2 μm thick SiO_2 layer was deposited via plasma-enhanced chemical vapor deposition. From the anisotropic Si wet etching characteristics, the wet etching rate in a hot KOH solution of [1-10] Si is faster than that of [111] Si or [11-2] Si; therefore, a hollow-structured microLED array could be fabricated. The microLED was arranged after the exposed Si region was etched to a depth of 1 μm, and the Si layer directly beneath the microLED was etched with a 40 wt% KOH solution heated to 80 °C. The Si layer was etched in the [1-10] direction at an etching rate of 2–3 μm min^{-1}. Figure 2(b) shows a bird's-eye-view of a scanning electron microscopy (SEM) image of the hollow-structured microLED array. It was necessary to retain the gate structure for attaining the hollow structure. Although only the result of 80×80 μm^2 microLEDs is presented, the effect of the microLED size on hollow structure formation was investigated in a preliminary experiment. As the Si etching was stopped once the (1-21) plane of Si was formed during the etching process, the success rate of hollow structure formation was reduced in microLEDs with sizes more than 100×100 μm^2. However, a hollow structure was successfully formed for all microLEDs with sizes 50×50 and 80×80 μm^2.

Subsequently, the collective microLED transfer method was investigated. For transferring onto a non-adhesive parylene film, a TR sheet with a simple control of the adhesive force (REVALPHA, Nitto Co. Ltd.) was used. The sheet was attached to a chip with a microLED array. The adhesion between the microLEDs and TR sheet was promoted by locally pressurizing the microLED array region on the TR sheet. On slowly removing the TR sheet from the chip, all the microLEDs were successfully transferred onto it. The TR sheet was then attached to a Si substrate with a 9 μm thick parylene film deposited on its surface. After applying a pressure of 50 kPa for 10 s, the sheet on the chip was heated at 150 °C for 1 min using a hot plate. This caused the loss of the adhesive force of the sheet, and the sheet was easily peeled off from the chip. Therefore, all microLEDs were simultaneously transferred onto the parylene film without rotation or misalignment. To ensure that the hollow structure formation and transfer process had not affected the microLED characteristics, the current–voltage characteristics of the microLEDs before KOH etching and after the transfer process were compared [Fig. 2(c)]. In both cases, similar rectification characteristics and bright blue emission were observed, suggesting that this process was suitable for fabricating a flexible microLED film. Parylene was deposited as an insulating layer on the film with the transferred microLED array. The parylene film of thickness 1 μm present on the n- and p-electrodes was removed by CF_4 and O_2 gas etching. Subsequently, a Ti/Au (50 nm/400 nm) metal wiring layer was deposited using an EB evaporator such that each microLED was driven independently. Finally, the surface of the microLED film was covered with a 1 μm thick parylene film for driving into the wet environment on the brain surface. The flexible microLED film was mounted on a printed circuit board with a compact design (15.5 mm × 14.3 mm) using flipchip bonding. The film was then manually peeled off from the base Si substrate.

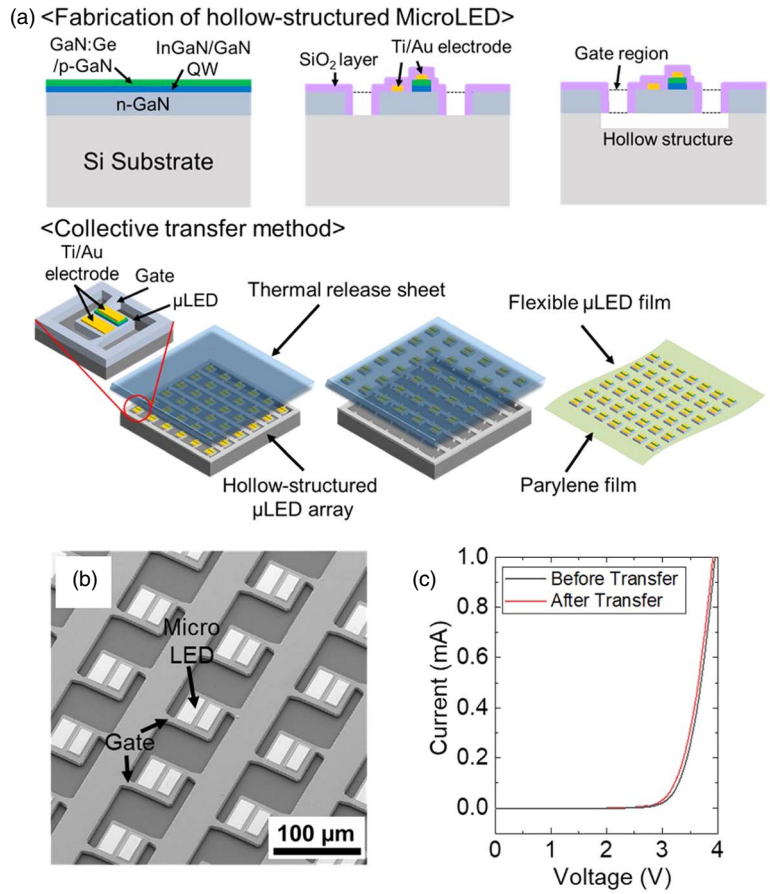

Fig. 2. (Color online) (a) Fabrication procedure of flexible microLED film. Upper illustration: Fabrication of hollow-structured microLED. Lower illustration: Collective transfer method. (b) Bird's-eye-view of the SEM image of hollow-structured microLED with size 80 × 80 μm^2. (c) Current–voltage characteristics of microLED before KOH solution etching and after transfer onto the parylene film.

Figure 3(a) shows the image of emission from the flexible microLED array film. Bright blue emission was observed from a single microLED by driving it independently, and its light pattern was obtained. Figure 3(b) shows the current-light output and external quantum efficiency (EQE) of this microLED, which were evaluated by the source measurement unit and the powermeter. A light output value of 22 mW mm^{-2}, corresponding with the value of 39.6 μW, was obtained at 0.5 mA (30 A cm^{-2}) with an EQE of 2.8%. For small animal experiments, temperature increase, ΔT, during the microLED drive is a major issue as it can cause the thermal stimulation of neural activity or even brain damage. According to the Association for the Advancement of Medical Instrumentation guideline, ΔT of a bioembedded device should not exceed 2 °C. Therefore, it is necessary to determine ΔT in advance before driving a microLED. Light output values in the range 0.1–1 mW mm^{-2} are required for ChR2 activation.[28,29] The required light output value from the microLED was determined by considering the distance between the microLED and the targeted neural cell; however,

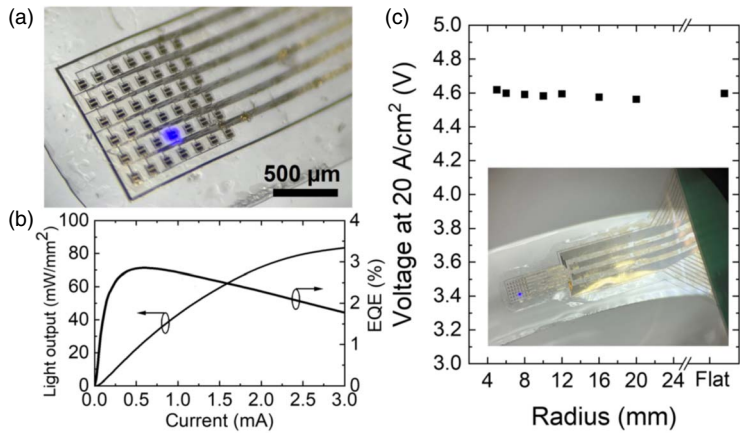

Fig. 3. (Color online) (a) Emission image of the flexible microLED array film. (b) Current-light output and EQE of a microLED on the flexible film. Light output value is 22 mW mm^{-2} at 0.5 mA (30 A cm^{-2}) with an EQE of 2.8%. (c) Voltage at 20 A cm^{-2} of microLED film as a function of the radius of curvature.

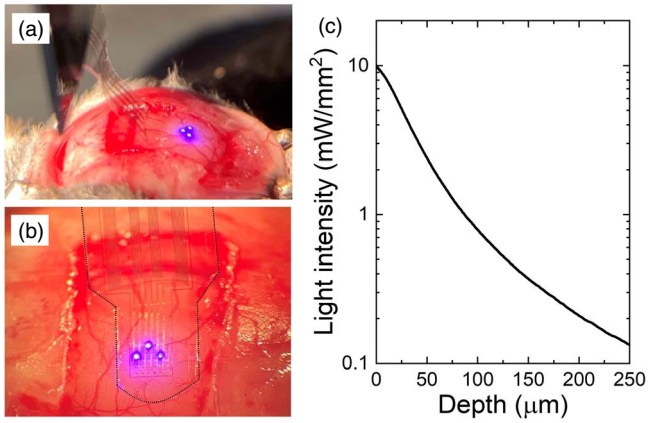

Fig. 4. (Color online) (a) Front and (b) top views of the flexible microLED array film on the brain surface. (c) Light attenuation characteristics in the brain as a function of depth.

the temperature increase was evaluated by assuming that a light output value of ~10 mW mm^{-2} was required. This value was obtained for a current of 0.25 mA (15 A cm^{-2}), and ΔT was determined to be 1.6 °C in air using a thermal camera. It is possible that ΔT was sufficiently reduced because the actual biological optical stimulation was performed on the brain surface during the pulse current drive. To investigate the effect of film bending on device characteristics, the current–voltage characteristics were obtained by attaching the film to cylinders with different curvature radii, ranging from 5 to 20 mm. The voltage as a function of the radius of curvature for 20 A cm^{-2} is shown in Fig. 3(c); microLED films showed negligible change in the drive voltage (<1%; 0.03 V).

The flexible microLED array film was placed on the surface of the cerebral cortex in a mouse (C57BL6/J), and the adhesion and luminescence were observed. Animal procedures were approved by the Animal Care and Use Committee of Dokkyo Medical University, and carried out in accordance with the guidelines of the National Institutes of Health. Figures 4(a) and 4(b) show the front and top views, respectively, of the flexible microLED array film on the cerebral cortex in an anesthetized mouse (isoflurane: 1.5%). The three microLEDs were simultaneously driven at 4.2 V, corresponding to a current of 80 μA (5 A cm^{-2}) for each microLED. As expected from the investigation of adhesion properties (Fig. 1), the film with a total thickness of 11 μm was sufficiently adhered to the brain, and three bright blue emission spots were observed. Finally, to understand the scope of the developed device, the extent of light penetration into the brain was examined. The light distribution of the microLED on the flexible film was evaluated by angle-resolved electroluminescence measurements, and the results showed a nearly Lambertian distribution. Based on this result, the light propagation through the brain tissue was simulated using the Monte Carlo method [Fig. 4(c)]. The scattering coefficient, anisotropy factor, and absorption coefficient of gray matter in cerebral cortex were $\mu_s = 105\,\mathrm{cm}^{-1}$, $g = 0.88$, and $\mu_a = 0.6\,\mathrm{cm}^{-1}$, respectively.[30] Typical light operation ranged from 0.1 to 1 mW mm^{-2},[28,29] and the region of the brain that was 100–250 μm away from the surface could be optically stimulated with a light output value of 10 mW cm^{-2}, which could sufficiently suppress heat generation. This indicates that the flexible microLED film would be effective for optogenetic stimulation.

In this study, a bioimplantable microLED array film capable of establishing suitable contact with the brain surface was developed for achieving optogenetic stimulation. The appropriate parylene film thickness was determined through a wrapping experiment for the realization of the microLED film. The fabrication technology of the hollow-structured microLED array and the collective transfer technology was established. Utilizing these technologies, a flexible microLED array film was successfully developed. There was no deterioration of the forward bias of the microLED during bending. Finally, blue emission that can sufficiently activate ChR2 was observed from the microLED film while it was in contact with the brain surface. The development of flexible microLED films can significantly contribute to the field of neuroscience research, particularly optogenetic research for the purpose of functional dissection of sub-regions on the brain surface, such as cerebral cortices, cerebellar lobules and olfactory system.

Acknowledgments This study was partially supported by the JST PRESTO (JPMJPR1885), Okinawa Institute of Science and Technology Kick-start fund, Murata Science Foundation, Daiko Foundation, Casio Science Promotion Foundation, Research Foundation for OptoScience and Technology, Takeda Science Foundation, and Tochigi Industrial Promotion Center (the Grant-in-Aid for World-Class Technological Research and Development). The fabrication processes were conducted at the facilities of the Electronics-Inspired Interdisciplinary Research Institute (EIIRIS), Venture Business Laboratory, and Toyohashi University of Technology.

ORCID iDs Hiroto Sekiguchi https://orcid.org/0000-0002-0692-9975

1) M. Rein et al., Nature **560**, 214 (2018).
2) R. X. G. Ferreira et al., IEEE Photonics Technol. Lett. **28**, 2023 (2016).
3) K. Kojima, Y. Yoshida, M. Shiraiwa, Y. Awaji, A. Kanno, N. Yamamoto, A. Hirano, Y. Nagasawa, M. Ippommatsu, and S. F. Chichibu, Appl. Phys. Lett. **117**, 031103 (2020).
4) J. Day, J. Li, D. Y. C. Lie, C. Bradford, J. Y. Lin, and H. X. Jiang, Appl. Phys. Lett. **99**, 031116 (2011).
5) J. G. Um, D. Y. Jeong, Y. Jung, J. K. Moon, Y. H. Jung, S. Kim, S. H. Kim, J. S. Lee, and J. Jang, Adv. Electron. Mater. **5**, 1800617 (2019).
6) K. Deisseroth, G. Feng, A. K. Majewska, G. Miesenböck, A. Ting, and M. J. Schnitzer, J. Nerurosci. **26**, 10380 (2006).
7) K. Deisseroth, Nat. Method **8**, 26 (2011).
8) T. Ishizuka, M. Kakuda, R. Araki, and H. Yawo, Neurosci. Res. **54**, 85 (2006).
9) Z. V. Guo, N. Li, D. Huber, E. Ophir, D. Gutnisky, J. T. Ting, G. Feng, and K. Svoboda, Neuron **81**, 179 (2014).
10) A. K. Dhawale, A. Hagiwara, U. S. Bhalla, V. N. Murthy, and D. F. Albeanu, Nat. Neurosci. **13**, 1404 (2010).
11) A. M. Packer, L. E. Rusell, W. P. Dalgleish, and M. Hausser, Nat. Methods **12**, 140 (2014).
12) T.-I. Kim et al., Science **340**, 211 (2013).
13) N. McAlinden, D. Massoubre, E. Richardson, E. Gu, S. Sakata, M. D. Dawson, and K. Mathieson, Opt. Lett. **38**, 992 (2013).
14) R. Scharf, T. Tsunematsu, N. McAlinden, M. D. Dawson, S. Sakata, and K. Mathieson, Sci. Rep. **6**, 28381 (2016).
15) F. Wu, E. Stark, P.-C. Ku, K. D. Wise, G. Buzsáki, and E. Yoon, Neuron **88**, 1136 (2015).
16) K. Kim, M. Vöröslakos, J. P. Seymour, K. D. Wise, G. Buzsáki, and E. Yoon, Nat. Commun. **11**, 2063 (2020).
17) H. Yasunaga, T. Takagi, D. Shinko, Y. Nakayama, Y. Takeuchi, A. Nishikawa, A. Loesing, M. Ohsawa, and H. Sekiguchi, Jpn. J. Appl. Phys. **60**, 016503 (2021).
18) M. A. Meitl, Z.-T. Zhu, V. Kumar, K. J. Lee, X. Feng, Y. Y. Huang, I. Adesida, R. G. Nuzzo, and J. A. Rogers, Nat. Method **5**, 33 (2005).
19) R. S. Cok et al., J. Soc. Inf. Disp. **25**, 589 (2017).

20) J.-H. Kim, B.-C. Kim, D.-W. Lim, and B.-C. Shin, J. Mech. Sci. Technol. **33**, 5321 (2019).
21) P. Delaporte and A.-P. Alloncle, Opt. Laser Technol. **78**, 33 (2016).
22) P. Serra and A. Pique, Adv. Mater. Technol. **4**, 1800099 (2018).
23) S.-C. Park, J. Fang, S. Biswas, M. Mozafari, T. Stauden, and H. O. Jacob, Adv. Mater. **26**, 5942 (2014).
24) S.-C. Park, J. Fang, S. Biswas, M. Mozafari, T. Stauden, and H. O. Jacob, IEEE J. Microelectromech. Syst. **24**, 1928 (2015).
25) D.-H. Kim et al., Nat. Mater. **9**, 511 (2010).
26) M. J. Chaudhury and G. M. Whitesides, Langmuir **7**, 1013 (1991).
27) B. Slischka, A. Nishikawa, and A. Loesing, Semiconductor Today **15**, 48 (2020).
28) E. Stark, T. Koos, and G. Buzsáki, J. Neurophysiol. **108**, 349 (2012).
29) N. Grossman et al., J. Neural Eng. **7**, 016004 (2010).
30) A. N. Yaroslavsky, P. C. Schulze, I. V. Yaroslavsky, R. Schober, F. Ulrich, and H.-J. Schwarzmaier, Phys. Med. Biol. **47**, 2059 (2002).